Interpretation of CEMP(s) and CEMP(s+r) stars with AGB models

Sara Bisterzo^{A,E}, Roberto Gallino^A, Oscar Straniero^B, Wako Aoki^{C,D}

Tokyo, 181-8588 Japan

Abstract: Asymptotic Giant Branch (AGB) stars play a fundamental role in the s-process nucleosynthesis during their thermal pulsing phase. The theoretical predictions obtained by AGB models at different masses, s-process efficiencies, dilution factors and initial r-enrichment, are compared with spectroscopic observations of Carbon-Enhanced Metal-Poor stars enriched in s-process elements, CEMP(s), collected from the literature. We discuss here five stars as example, CS 22880-074, CS 22942-019, CS 29526-110, HE 0202-2204, and LP 625-44. All these objects lie on the main-sequence or on the giant phase, clearly before the TP-AGB stage: the hypothesis of mass transfer from an AGB companion, would explain the observed s-process enhancement. CS 29526-110 and LP 625-44 are CEMP(s+r) objects, and are interpreted assuming that the molecular cloud, from which the binary system formed, was already enriched in r-process elements by SNII pollution. In several cases, the observed s-process distribution may be accounted for AGB models of different initial masses with proper 13 C-pocket efficiency and dilution factor. Na (and Mg), produced via the neutron capture chain starting from 22 Ne, may provide an indicator of the initial AGB mass.

Keywords: stars: AGB — Carbon — Population II

1 Introduction

A sample of about one hundred of C–rich, s–rich is marginally activated during the convective thermal metal–poor (CEMPs) and, when detected, lead–rich stars have been observed in recent years (see Sneden, Cowan, 25 GLOSINK. This maximum temperature slightly increases with pulse number and decreasing the metal-

Observed halo stars are of low mass $(M \leq 0.9~M_{\odot})$ and long lifetimes, with effective temperatures and surface gravities characteristic of main—sequence stars, subgiants or giants, far from the Asymptotic Giant Branch (AGB) phase where the s-process is manufactured. Therefore, the hypothesis of mass accretion of s-rich material from a more massive AGB companion, becomes essential to explain the overabundances detected in their spectra.

Our aim is to interpret the spectroscopic data of CEMP-s stars with AGB theoretical models using different 13 C-pocket efficiencies and initial masses. Stellar model parameters have been derived over a set of AGB models obtained with the FRANEC code, as discussed in Straniero et al. (2003). Neutrons are released by the two reactions 13 C(α , n) 16 O and 22 Ne(α , n) 25 Mg. The first reaction is the major neutron source. When the H-shell is inactive, the so called Third Dredge–Up (TDU) episode permits partial mixing processes between material of the He–inter-shell and the convective envelope. During the TDU, few protons are assumed to penetrate into the top layers of the He–intershell, and subsequently react via 12 C(p, γ) 13 N(β + ν) 13 C chain, enriching in 13 C a thin region at the top of the He–intershell, the 13 C-pocket. At $T\sim0.9\times10^8$

K, 13 C burns radiatively during the interpulse period (Straniero et al. 1995). The second neutron source is marginally activated during the convective thermal pulses, when the maximum temperature reaches $T > 25 \, \text{CMMnK}$. This maximum temperature slightly increases with pulse number and decreasing the metallicity (see Cristallo et al. 2009). Although this second neutron burst represents only a few percent of the total neutron exposure, it modifies the abundance patterns of several branchings that are sensitive to temperature and neutron density.

Observations of s—enhanced stars at various metallicities require a range of s—process efficiencies (Sneden, Cowan, & C2008). Starting from the ST case¹, which has been shown to reproduce the solar main component for AGB models of half-solar metallicity (Arlandini et al. 1999), we consider a large range of $^{13}\mathrm{C}$ —pocket efficiencies between ST/60 up to ST×2.

The s-process is characterized by three abundance peaks, the Zr-peak (light-s, ls), the Ba-peak (heavy-s, hs), and the Pb-peak at the termination of the s-process path, corresponding to the magic neutron numbers $N=50,\,82,\,126.$ We adopt the spectroscopic definition [ls/Fe] = $\log_{10}(\text{ls/Fe})_{\star}$ - $\log_{10}(\text{ls/Fe})_{\odot}$ and analogously for [hs/Fe] and [Pb/Fe]. We assume ls = (Y,Zr) and hs = (La,Nd,Sm), because Sr and Ba have few and saturated lines (see Busso et al. 1995). To characterize the whole s-process distribution, two s-process

^A Dipartimento di Fisica Generale, Università di Torino, via P. Giuria, 1, 10125 Torino, Italy

^B INAF Osservatorio Astronomico di Collurania, via M. Maggini, 64100 Teramo, Italy

^C National Astronomical Observatory of Japan, 2-1-21 Osawa, Mitaka, Tokyo, 181-8588 Japan

 $^{^{\}mathrm{D}}$ Department of Astronomical Science, The Graduate University of Advanced Studies, Mitaka,

^E Email: bisterzo@ph.unito.it

¹Our ¹³C-pocket extend in mass for 9.4×10^{-4} M_{\odot} (about 1/20 of the typical mass involved in a TP), and contains 4.7×10^{-6} M_{\odot} of ¹³C (ST case).

indicators, [hs/ls] and [Pb/hs], independent of the specific envelope abundance enhancement, are necessary. The spectroscopic s-process abundances observed in CEMP(s) stars depend on the fraction of the AGB mass transferred by stellar winds, whilst the s-process indicators [hs/ls] and [Pb/hs] remains unchanged. We may introduce a dilution factor between the AGB mass transferred and the original envelope of the observed star. We will define the logarithmic ratio 'dil' as

dil = $\log \left(\frac{M_{\star}^{\text{env}}}{\Delta M_{\star}^{\text{trans}}} \right)$, where M_{\star}^{env} represents the mass of the convective envelope of the observed star before the mixing, and ΔM_{AGB}^{trans} is the AGB total mass transferred. For instance, dil ~ 0 dex means that the convective envelope mass of the observed star, which was interested in the mixing processes, is of the same order of the s-rich material transferred from the AGB. Lowmetallicity main sequence stars, with mass of about 0.8 $-0.9 M_{\odot}$, are characterized by a very thin convective subphotospheric layer $(M \le 10^{-3} M_{\odot})$. Instead, for a giant that already suffered the first dredge-up (FDU) episode, the convective envelope extends to 8/10 of the mass of the star. For subgiants, different degrees of FDU deepness can be reached, and a range of dilution factors can be adopted.

For halo stars, an initial α -enhancement of $[\alpha/\text{Fe}]$ = 0.3 - 0.5 dex is adopted for Mg, Si, Ca, and Ti. As for [O/Fe], we adopt a linear increase with decreasing metallicity: $[O/Fe] = -0.4 \times [Fe/H]$ according to Abia et al. (2001). Furthermore, during the AGB phase, a primary contribution to ¹⁶O derives from the partial He-burning during the thermal pulses, through $^{12}{\rm C}(\alpha,\gamma)^{16}{\rm O}$.

Many CEMP(s) stars are also enriched in r-process elements, CEMP(s+r). About 70% of solar La is synthe sized by the s-process (Winckler et al. 2006), whilst 94% of solar Eu is provided by the r-process. [La/Eu] is the major indicator of s + r enrichment in stars. The theoretical AGB predictions from a pure main s-process give $[La/Eu]_s \sim 1$. The r-process elements are not synthesized by AGBs; consequently in order to explain much lower observed [La/Eu] ratio (down to 0), different scenarios have been proposed in the literature². Vanhala & Cameron (1998) showed through numerical simulations how Type II supernova ejecta may interact with a molecular cloud, polluting it with freshly synthesized material (in particular r-process), likely triggering the formation of binary systems, which consists of stars with low mass. We assume that the molecular cloud, from which the binary system formed, was pre-enriched in r-elements because of supernova Type II pollution (Bisterzo et al. 2008a,b; Sneden, Cowan, &hGallindan the other two r-process elements [Eu/Fe] 2008). Our choice of the initial r-rich element abundances was made considering the r-process solar predictions from Arlandini et al. (1999), taking into account the different $r{\rm -process}$ percentage to solar abundances that contributes to each isotope of a given ele-

Two papers are in preparation that will describe accurately the AGB theoretical models and interpret the abundances of all CEMP(s) and CEMP(s+r) stars discovered so far. The aim of this paper is to discuss five of these objects as specific examples: the main-sequence/turnoff star CS 29526-110, the subgiant CS 22880-074 (Sect.2), and the three giants, CS $22942{-}019$ (Sect.2), LP 625 ${-}44,$ and HE 0202 ${-}2204.$ For HE 0202-2204 no lead is measured and we provide a theoretical prediction (Sect.4). Two of the five stars, CS 29526-110 and LP 625-44, are CEMP(s+r) (Sect.3).

2 CEMP(s) stars

The subgiant CS 22880-074 ($T_{\rm eff}=5850~{
m K}$ and $\log g = 3.8$; [Fe/H] = -1.93) analyzed by Aoki et al. (2002c,d), with a mild s-process enhancement: [ls/Fe] ~ 0.3 , [hs/Fe] ~ 1.2 , and [Pb/Fe] ~ 1.9 . Aoki et al. (2007) reported a subsolar [Na/Fe], including NLTE corrections (-0.7 dex for this object). The ratios [hs/ls] and [Pb/hs] observed give an indication of the whole s-process distribution. The difference between the predicted [La/Fe] by an AGB model and the one observed in CS 22880-074 gives a first assessment of the dilution of the AGB material, afterward optimized with a more careful analysis of the uncertainties of the singles species. The goodness of the fit is tested for different AGB masses by considering all the elements from carbon to lead, weighing the number of lines detected for each of them. The lower initial mass modeled ($M_{\rm ini}^{\rm AGB}=1.2~M_{\odot}$ with only three thermal pulses followed by TDU) and a case ST/9, predicts [La/Fe]_{th} = 1.47 at $[Fe/H]_{th}$ = -2: no solutions are possible for this star without a dilution factor because of the low s-enhancement.

We show in Fig. 1 the two theoretical interpretations for this star using $M_{\rm ini}^{\rm AGB}=1.2~M_{\odot}$, a case ST/9 and dil = 0.45 dex (red line), and $M_{\rm ini}^{\rm AGB}=$ $1.3~M_{\odot}$, a case ST/6 and dil = 0.85 dex (blue dotted line). The predicted $[N/Fe] \sim 0.8$ by these models, takes into account the typical enhancement of \sim 0.6 dex due to the FDU, and the additional contribution from the H-shell ashes mixed with the envelope during the TDU. This second contribution increases with the number of thermal pulses. AGB models of higher initial mass ($M_{\rm ini}^{\rm AGB}=1.5$ and 2 M_{\odot} , with dil = 1.75 and 2.2 dex, respectively) would reproduce [hs/Fe] and [Pb/Fe], but overestimated of ~ 0.5 dex the observed [Y/Fe] (no zirconium is detected in this star), and similarly for [Na/Fe]. The observed [La/Eu] ratio is in agreement with a pure s-process contribution $([r/Fe]^{ini} = 0$, which corresponds to [La/Eu] = 0.8 for the case shown in Fig. 1). [Er/Fe] is about 0.5 dex and $[Dy/Fe]^3$.

No radial velocity variations were measured for CS 22880-074 (Preston & Sneden 2001; Aoki et al. 2002c). Preston (these Proceedings) confirms the non-detection of velocity variations with his data over a period of 16 years. This is not a stringent argument against binarity (see also Tsangarides 2005).

The giant CS 22942-019 was analyzed by Aoki et al. (2002c,d) and Schuler et al. (2008).

²See Jonsell et al. (2006) and references therein.

³Note that for Eu, Dy and Er only one line is detected.

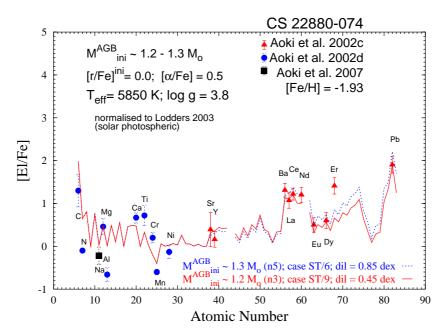


Figure 1: Comparison of the [El/Fe] abundances of CS 22880–074 by Aoki et al. (2002c,d, 2007), with AGB stellar models of 1.2 and 1.3 M_{\odot} , ST/6 and ST/9, and dil = 0.45 and 0.85 dex, respectively. All the data and the theoretical expectations are normalized to the solar photospheric abundances by Lodders (2003).

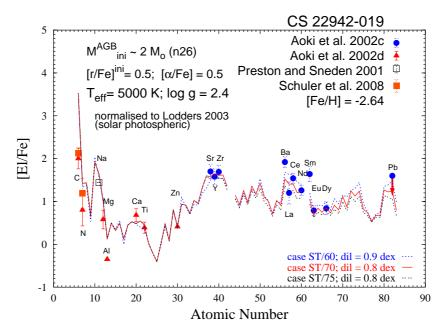


Figure 2: Comparison of the [El/Fe] abundances of CS 22942-019 by Aoki et al. (2002c,d, 2007) and Schuler et al. (2008) using AGB stellar models of 2 M_{\odot} , ST/60, ST/70 and ST/75, and dil = 0.8 – 0.9 dex.

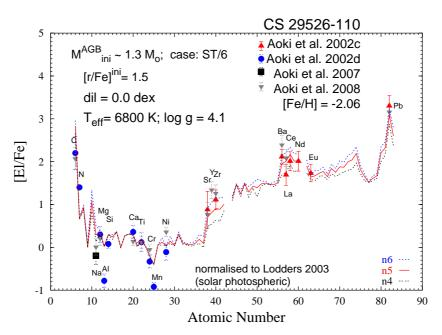


Figure 3: Comparison of the [El/Fe] abundances of CS 29526–110 by Aoki et al. (2002c,d, 2007, 2008), with AGB stellar models of 1.3 M_{\odot} , ST/6, and [r/Fe]ⁱⁿⁱ = 1.5. The envelope overabundances after the fourth, fifth and sixth thermal pulse are shown (n4, n5, n6), corresponding to an uncertainty of the initial AGB mass (\pm 0.05 M_{\odot}).

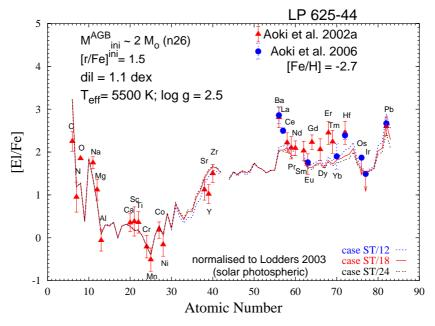


Figure 4: Comparison of the [El/Fe] abundances of LP 625–44 by Aoki et al. (2002a, 2006), with AGB stellar models of 2 M_{\odot} , ST/12, ST/18, ST/24, and dil = 1.1 dex. Note that the observed [O/Fe] is very uncertain in this star (see Aoki et al. 2002a).

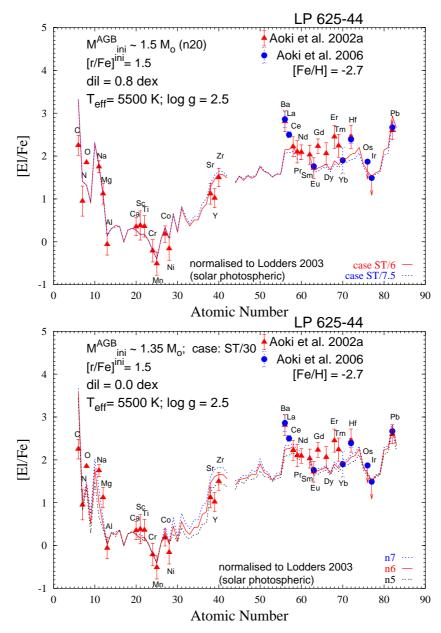


Figure 5: The same as Fig. 4, but with AGB stellar models 1.5 M_{\odot} , ST/6, ST/7.5 and dil = 0.8 dex (top panel) and 1.35 M_{\odot} , ST/30 and dil = 0.0 dex (bottom panel).

Preston & Sneden (2001) derived its period, $505 d \le P$ ≤ 3125 d, discovering it is a long period binary. A very high [Na/Fe] = 1.44 was found by Preston & Sneden (2001). For elements belonging to the hs peak, we expect differences in the predictions at most of Δ [hs/Fe] ~ 0.2 dex, in disagreement with the observed [Ba/La] = 0.7 ± 0.2 . Ce and Nd abundances appear to be more reliable with 6 and 7 lines, while Ba, La and Sm have 3, 2 and 1 lines, respectively. Only an upper limit for lead is available ($[Pb/Fe] \le 1.6$ and $[Pb/hs] \le$ 0), suggesting AGB models with a low s-process efficiency. For $M_{\rm ini}^{\rm AGB}=2~M_{\odot}$ and a case ST/70 (Fig. 2), a dil = 0.8 - 0.9 dex is applied, in agreement with a giant after the FDU episode. The high predicted [Na/Fe] is derived from $^{22}{\rm Ne}({\rm n},\gamma)^{23}{\rm Na}$. Concerning [Mg/Fe], one has to take account of the initial enhancement of ²⁴Mg and of the additional contribution by the 23 Na(n, γ) 24 Mg reaction; moreover, a very high overabundance of 25 Mg and 26 Mg is produced via $^{22}\mathrm{Ne}(\alpha,\mathrm{n})^{25}\mathrm{Mg}$ and $^{22}\mathrm{Ne}(\alpha,\gamma)^{26}\mathrm{Mg}$, and by neutron captures. With low initial mass cases a lower dilution would be required (dil = 0.5 dex for $M_{\rm ini}^{\rm AGB} = 1.5~M_{\odot}$ and no dilution for $M_{\rm ini}^{\rm AGB} = 1.35~M_{\odot}$ model). A higher mass model, $M_{\rm ini}^{\rm AGB} = 3~M_{\odot}$, has to be excluded, because to reproduce [hs/Fe] and [Pb/Fe] a dil ~ 1.0 dex is required, whilst [ls/Fe] (as well as Na and Mg) would be overestimated.

$3 \quad \text{CEMP(s+r) stars}$

Among the objects with Eu detected, sixteen stars are CEMP(s+r)⁴ ($\sim 40\%$), five of them showing a very high initial r-enrichment ([r/Fe]ⁱⁿⁱ = 2.0; see Sneden, Cowan, & Gallino 2008). In this Section, we discuss the two stars CS 29526-110 and LP 625-44.

CS 29526–110 has been analyzed several times (Aoki et al. 2002c,d, 2007, 2008). It is a single–lined binary (Aoki et al. 2002d; Tsangarides 2005), although its period remains uncertain. This object appears to be a turnoff star or a slightly evolved subgiant ($T_{\rm eff}=6500\pm200$ K, log $g=3.2\pm0.5$).

The theoretical interpretation shown in Fig. 3 corresponds to an AGB model of $M_{\rm ini}^{\rm AGB}=1.3~M_{\odot}$, case ST/6 and no dilution factor. Nitrogen abundance is very uncertain, because of the difficulty of the CN band detection. The observed [Na/Fe] is about solar (Aoki et al. 2007, 2008). The most recent La measurement (Aoki et al. 2008) better agrees with the prediction. With a higher initial AGB mass models ($M_{\rm ini}^{\rm AGB} \ge 1.4~M_{\odot}$), Na and Mg are overestimated, whilst the s-process elements are would be reproduced with a proper dilution and $^{13}{\rm C-pocket}$ case. The [La/Eu] \sim 0.3 suggests an initial r-process enrichment [r/Fe]ⁱⁿⁱ = 1.5, while a pure s-process model would predict [La/Eu]_{th} = 0.85.

Aoki et al. (2002a) carried out a detailed analysis of the s+r-rich subgiant **LP 625-44**, subsequently improved by determining the upper limits for two r-process elements, Os and Ir (Aoki et al. 2006).

The binarity of this object was confirmed by radial velocity monitoring (Norris, Ryan, & Beers 1997; Aoki et al. 2000), strongly supporting the mass transfer scenario, but the period has not been detected yet. Very enhanced Na and Mg are observed in this star ([Na/Fe] = 1.75; [Mg/Fe] = 1.12). With $M_{\text{ini}}^{\text{AGB}} = 2 M_{\odot}$ (Fig. 4), ST/18 and dil = 1.1 dex, we find a reasonable solution for all s-elements, and [Na/Fe] is acceptable within 2σ uncertainty. Remember that Na is affected by the poorly understood corrections due to 3D atmospheric analysis and non-LTE calculation (Aoki et al. 2008). The observed [Pb/hs] ratio is low (~ 0.35 dex), and a low neutron flux (ST/18) is needed to interpret the whole s-process pattern. Also for $M_{\rm ini}^{\rm AGB}=1.5~M_{\odot},$ ST/6 and ST/7.5, and dil = 0.8 dex, a satisfactory solution found (Fig. 5, top panel). In Fig. 5, bottom panel, we extend to the light elements the solution already presented in Aoki et al. (2006) for a $M_{\rm ini}^{\rm AGB}$ = $1.35~M_{\odot}$ model. However, in this case [Na/Fe] and [Mg/Fe] would be underestimated. [Y/Fe] is lower than the theoretical results - note that we predict differences of at most the order of 0.2 dex between [Y/Fe] and [Zr/Fe] – while [Ba/Fe] and [La/Fe] are both underestimated by the model. We considered Ce as more reliable among the second s-peak with 33 lines detected, while 4 and 13 lines are used for Ba and La, respectively. To match the r-process abundances, we used an initial r-enrichment $[\hat{r}/\text{Fe}]^{\text{ini}} = 1.5 \text{ dex.}$ This choice is consistent with the upper limits of Os and Ir.

4 Lead predictions

For several stars among CEMP(s) and CEMP(s+r), no lead is measured, and we give our theoretical predictions. In some cases, due to the uncertainty of the spectroscopic observations, we can only hypothesize a range of expectations.

As example we discuss here **HE 0202–2204** studied by Barklem et al. (2005). This giant can be interpreted with all the initial masses in the range $M_{\rm ini}^{\rm AGB}$ = 1.3 and 2 M_{\odot} , adopting low ¹³C–pockets (ST/9 and ST/6) and dil = 0.8 and 2.0 dex, respectively (Fig. 6). The lead predicted is [Pb/Fe]_{th} ~ 2.1. All the s-process elements are well matched.

5 Conclusions

We analyzed the AGB model results for different initial masses $(M_{\rm ini}^{\rm AGB}=1.3,~1.4,~1.5,~2~{\rm and}~3~M_{\odot}),$ metallicities $(-3.6 \leq {\rm [Fe/H]} < -1)$ and $s{\rm -process}$ efficiencies (ST/150 $\leq {\rm ^{13}C-pocket} \leq {\rm ST} \times 2),$ and tested these models through a comparison between theoretical predictions and spectroscopic abundances of the five CEMP(s) and CEMP(s+r) stars: CS 22880–074, CS 22942–019, CS 29526–110, HE 0202–2204, and LP 625–44. By comparing the [Na/Fe] (and [Mg/Fe]) observations with theoretical models, we can obtain an indicator of the initial AGB mass (Bisterzo et al. 2006). For instance, the low [Na/Fe] observed in CS 22880–074 and CS 29526–110 may be interpreted with $M_{\rm ini}^{\rm AGB} \sim 1.3~M_{\odot}$ models. However, a large uncertainty affects Na due to poorly understood NLTE effects and

 $^{^{4}}$ We classified a stars as CEMP(s+r) if [r/Fe]ⁱⁿⁱ \geq 1, where [r/Fe]ⁱⁿⁱ is the initial r-enhancement assumed to interpret the observations.

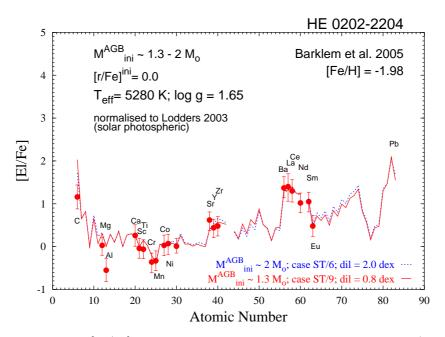


Figure 6: Comparison of the [El/Fe] abundances of HE 0202–2204 by Barklem et al. (2005), with a AGB stellar models of 1.3 and 2 M_{\odot} , ST/9 and ST/6, and dil = 0.8 and 2.0 dex, respectively. We predict [Pb/Fe]_{th} \sim 2.1.

Table 1: Metallicity, atmospheric parameters, evolutionary stage (MS means main—sequence star; SG means subgiant; G means giant), and some of the observed elements for the five stars analyzed. In column 6, stars after the FDU are labeled as 'yes', and viceversa 'no'.

Star	$[\mathrm{Fe/H}]$	$T_{\rm eff}$	$\log g$	Type	FDU	[Na/Fe]	$[\mathrm{Mg}/\mathrm{Fe}]$	[ls/Fe]	$[\mathrm{hs/Fe}]$	$[\mathrm{Pb}/\mathrm{Fe}]$
CS 22880-074	-1.93	5850	3.8	SG	no	-0.09	0.46	0.16	1.14	1.90
CS 22942-019	-2.64	5000	2.4	G	yes	1.44	0.58	1.64	1.37	≤ 1.6
CS 29526-110	-2.06	6800	4.1	MS	no	-0.07	0.22	1.11	1.85	3.30
HE 0202-2204	-1.98	5280	1.65	G	yes	-	-0.01	0.44	1.14	-
LP 625-44	-2.70	5500	2.5	G	yes	1.75	1.12	1.26	2.21	2.67

Table 2: Summary of the theoretical interpretations for the five stars analyzed.

Star	$M_{ m ini}^{ m AGB}$	¹³ C-pocket	dil	$[r/Fe]^{ini}$	Fig.
CS 22880-074	1.2	ST/9	0.5	0.0	1
-	1.3	ST/6	0.8	0.0	1
CS 22942-019	1.35	ST/75	0.0	0.5	-
-	2	ST/70	0.8	0.5	2
CS 29526-110	1.3	ST/6	0.0	1.5	3
HE $0202-2204$	1.3	ST/9	0.8	0.0	6
-	1.5	ST/4	1.6	0.0	-
-	2	ST/6	2.0	0.0	6
LP 625-44	1.35	ST/30	0.0	1.5	5, top panel
-	1.5	ST/6	0.8	1.5	5, bottom panel
-	2	ST/18	1.1	1.5	4

for 3D atmospheric models. Another indicator of the initial AGB mass is the ls peak, since the [ls/Fe] ratio is more sensitive to the thermal pulse number. Solutions in the range of $1.3 \leq M_{\rm ini}^{\rm AGB}/M_{\odot} \leq 2$ are accepted.

in the range of $1.3 \leq M_{\rm ini}^{\rm AGB}/M_{\odot} \leq 2$ are accepted. For CEMP(s+r) stars, we suggest that the molecular cloud, from which the binary system was formed, was pre-enriched in r-elements because of pollution by Type II supernovae. Different initial r-process enrichments are adopted to explain the observations. The two CEMP(s+r) stars discussed here, CS 29526-110 and LP 625-44, need an initial r-enrichment of [r/Fe] ini = 1.5

The discrepancies between observed and predicted C and N can be explained by efficient Cool Bottom Processing (CBP), a mixing process which occurs in low—mass stars (Nollett, Busso, & Wasserburg 2003; Wasserburg et al. 2006). This process may decrease significantly the C abundance in the envelope, while N increases.

In Table 1 the major observational characteristics of the five stars discussed in this work are reported, and in Table 2 the corresponding theoretical interpretation are presented.

Two forthcoming papers will extend the analysis to the full sample of 85 CEMP(s) stars, with a detailed presentation of the AGB stellar models, including intermediate mass AGBs, and the data tables of the theoretical results with metallicity and s-process efficiency changes.

A final consideration has to be mentioned. For $[{\rm Fe/H}] \leq -2.5$ and mass $M_{\rm ini}^{\rm AGB} \leq 1.5~M_{\odot}$, a peculiar phenomenon has been advanced: an anomalous proton ingestion episode (PIE), from the envelope down to the convective He–intershell, occurs during the first TDU (see Cristallo et al. 2009, and references therein). The consequence is a huge TDU episode affecting the s–process distribution.

Acknowledgments

We thank the anonymous Referee for insightful comments, which have helped improving the paper. Work supported by the Italian MIUR—PRIN 2006 Project 'Late Phases of Stellar Evolution: Nucleosynthesis in Supernovae, AGB Stars, Planetary Nebulae.'

References

- Abia, C., Busso, M., Gallino, R. et al. 2001, ApJ, 559, 1117
- Aoki, W., Beers, T. C., Sivarani, T., et al. 2008, ApJ, 678, 1351
- Aoki, W., Beers, T., Christlieb, N., et al. 2007, ApJ, 655, 492
- Aoki, W., Bisterzo, S., Gallino, R., et al. 2006, ApJ, 650, 127
- Aoki, W., Ando, H., Honda, S., et al. 2002a, Publ. Astron. Soc. Japan, 54, 427

- Aoki, W., Norris, J. E., Ryan, S. G., Beers, T. C., Ando, H. 2002c, Publ. Astron. Soc. Japan, 54, 933
- Aoki, W., Ryan, S. G., Norris, J. E., et al. 2002d, ApJ, 580, 1149
- Aoki, W., Norris, J. E., Ryan, S. G., Beers, T. C., Ando, H. 2000, ApJ, 536, 97
- Arlandini, C., Käppeler, F., Wisshak, K., et al. 1999, ApJ, 525, 886
- Barklem, P. S., Christlieb, N., Beers, T. C., et al. 2005, A&A, 439, 129
- Bisterzo, S., Gallino, R., Straniero, O., et al. 2008a, AIP Conf. Proc., 990, 330
- Bisterzo, S., Gallino, R., Straniero, O., et al. 2008b, AIP Conf. Proc. 1001, 131
- Bisterzo, S., Gallino, R., Straniero, O., et al. 2006, AIP Conf. Proc., 847, 368
- Busso, M., Lambert, D. L., Beglio, L., et al. 1995, ApJ, $446,\,775$
- Cristallo, S., Piersanti, L., Straniero, O., Gallino, R., Domínguez, I., Käppeler, F. 2009, PASA, in press
- Jonsell, K., Barklem, P. S., Gustafsson, B., et al. 2006, A&A, 451, 651
- Lodders, K. 2003, ApJ, 591, 1220
- Nollett, K. M., Busso, M., & Wasserburg, G.J. 2003, ApJ, 582, 1036
- Norris, J. E., Ryan, .G., & Beers, T. C. 1997, ApJ, $488,\,350$
- Preston, G. W., & Sneden, C. 2001, AJ, 122, 1545
- Schuler, S. C., Margheim, S. J., Sivarani, T. et al. 2008, AJ, 136, 2244
- Sneden, C., Cowan, J. J., & Gallino, R. 2008, ARA&A, 46, 241
- Straniero, O., Domínguez, I., Cristallo, S., Gallino, R. 2003, PASA, 20, 389
- Straniero, O., Gallino, R., Busso, M., et al. 1995, ApJ, 440, 85
- Tsangarides, S. A. 2005, Ph.D. Thesis, Open University (United Kingdom), DAI-C 66/04
- Vanhala, H. A. T. & Cameron, A. G. W. 1998, ApJ, 508, 291
- Wasserburg, G. J., Busso, M., Gallino, R., Nollett, K. M. 2006, Nucl. Phys. A, 777, 5
- Winckler, N., Dababneh, S., Heil, M., et al. 2006, ApJ, 647, 685